Lee, Pedro Jose; Vitkovsky, John; Lambert, Martin Francis; Simpson, Angus Ross; Liggett, James A. Discrete blockage detection in pipelines using the frequency response diagram: Numerical study Journal of Hydraulic Engineering, 2008; 134 (5):658-663

Discrete Blockage Detection in Pipelines Using the Frequency Response Diagram: Numerical Study

Pedro J. Lee[1]; John P. Vitkovský[2]; Martin F. Lambert[3]; Angus R. Simpson[4]; and James A. Liggett[5]

[1]Lecturer, Dept. of Civil and Natural Resources Engineering, College of Engineering, Univ. of Canterbury, Private 4800, Christchurch, 8020, New Zealand. E-mail: Pedro.lee@canterbury.ac.nz

[2]Hydrologist, Water Assessment Group, Dept. of Natural Resources and Water, Queensland Government, Indooroopilly QLD 4068, Australia. E-mail: john.vitkovsky@nrw.qld.gov.au

[3]Associate Professor, Centre for Applied Modelling in Water Engineering, School of Civil and Environmental and Mining Engineering, Univ. of Adelaide, Adelaide SA 5005, Australia. E-mail: mlambert@civeng.adelaide.edu.au

[4]Professor, School of Civil, Environmental and Mining Engineering, Univ. of Adelaide, Adelaide SA 5005, Australia. E-mail: asimpson@civeng.adelaide.edu.au

[5]Professor Emeritus, School of Civil and Environmental Engineering, Cornell Univ., Ithaca, NY 14853-3501. E-mail: jal8@cornell.edu

Abstract: This paper proposes the use of fluid transients as a noninvasive technique for locating blockages in transmission pipelines. By extracting the behavior of the system in the form of a frequency response diagram, discrete blockages within the pipeline were shown to induce an oscillatory pattern on the peaks of this response diagram. This pattern can be related to the location and size of the blockage. A simple analytical expression that can be used to detect, locate, and size discrete blockages is presented, and is shown able to cater for multiple blockages existing simultaneously within the system. The structure of the expression suggests that the proposed technique can be extended to situations where system parameters may not be known to a high accuracy and also to more complex network scenarios, although future studies may be required to verify these possibilities.

Keywords: Frequency response; Linear systems; Transients; Water pipelines; Resonance; Numerical analysis.

Introduction

The increasing industrial reliance on pipeline systems for the transport of materials has led to the recent emphasis on technologies for the fast detection and location of faults within such systems. Amongst the types of problems that can occur in a pipeline system, the formation of blockages within the pipe poses a most elusive problem for existing fault detection technologies. Unlike leaks within piping systems, a blockage does not generate clear external indicators for its location such as the release and accumulation of fluids around the pipe. Often intrusive procedures, such as the insertion of a closed-circuit camera or a robotic pig, are required to determine the location of blockages. The creation of nonintrusive techniques for fault detection that gives a clear picture of the internal conditions of the pipeline is desirable, and the use of fluid transients for this purpose is a promising development.

Fluid transients are modified by the conditions within the pipeline. The behavior of these transient waves can be used to indicate the internal condition of the pipe system. There has been a range of publications proposing different strategies of fluid transient usage in leak detection and these methods share a common theme in that a small amplitude disturbance—a fluid transient—is injected into a pipe and the subsequent pressure response is measured and analyzed to derive system information. This type of analysis is more commonly known as system response extraction and forms the basis of well-established methodologies used to extract dynamic responses of complex mechanical and electrical systems.

The behavior of any system can be summarized by a frequency response diagram (FRD) that describes how the system affects each individual frequency component of the injected transient signal. Under the influence of transients pipeline systems display near linear behavior and the FRD is defined as

$$H(\omega) = \frac{\Im\{y(t)\}}{\Im\{x(t)\}} \quad (1)$$

where $H(\omega)$ frequency response function; $\Im =$ Fourier transform of the functions *x(t)* and *y(t)*, which stand for input and output, respectively (Lynn 1982); ω = frequency; and t = time. The input to the system is given by the nature of the injected transient signal (e.g., the induced discharge variation at the transient generating valve due to the valve movement), and the output is given by the measured head response from the pipe.

The medical field was among the first to use the FRD of pipe-like systems for measurement in the human vocal tract (Schroeder 1967; Mermelstein 1967; De Salis and Oldham 2001). These techniques rely on the measured shifts in the resonant frequencies of the pipeline system for the detection of extended blockages within gas transmission pipeline systems. Unless the extent of the blockage is substantial in relation to the scale of the pipeline system, these shifts in the resonant frequencies are often not perceptible in water pipes. For mild blockages in large systems, the blockage can be considered as discrete, similar to that generated by a partially closed inline valve.

There has been recent work into the use of the FRD for detecting blockages in liquid pipelines (Wang et al. 2005; Mohapatra et al. 2006; Lee and Vitkovský 2006), but the effect of a discrete blockage on the FRD has not been quantified. In this paper an analytical expression is derived that allows discrete blockages to be detected within a single pipeline system using the shape of the FRD. In a clear pipeline system without blockages, the FRD has a series of resonant peaks that decay smoothly with frequency due to unsteady frictional damping (Vitkovský et al. 2003). A discrete blockage within the system results in an oscillatory pattern being imposed on the resonant peak magnitudes. This is illustrated in a numerical example using the pipeline in Fig. 1.

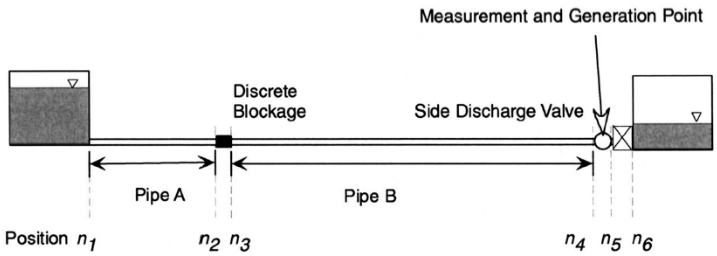

Figure 1: Pipeline system under consideration

The numerical example system in Fig. 1 consists of a 2,000 m length of a 0.3 m diameter pipeline and is bounded by constant head reservoirs. The heads for the upstream and downstream reservoirs are 50 and 20 m, respectively. There is a fully opened inline valve at the downstream end of the system, with a valve loss coefficient, C_V=0.002 $m^{5/2}$ s^{-1}. The wave speed of the system is 1,200 m s^{-1} and the transient is generated by the perturbation of a side discharge valve located just upstream of the inline valve. The impedance of the blockage, $I_B=\Delta H_{B0}/Q_{B0}$=763.9 m^{-2} s and the dimensionless location of the blockage is defined as

$$x_b^* = \frac{L_A}{L_A + L_B} \tag{2}$$

where L_A, L_B=length of the pipe section A and section B as indicated in Fig. 1. The size of the blockage can be expressed in dimensionless form as $I_B^* = I_B/B$, where *B=a/gA* and is the characteristic impedance of the pipe. The dimensionless blockage size for this case is $I_B^* = 0.44$. This blockage size was purposely made large to clearly shown the impact of a blockage on the FRD. For the purpose of isolating the impact of the blockage on the FRD, the pipeline is assumed to be frictionless. The impact of steady friction reduces the magnitude of the FRD peaks uniformly and does not change the pattern induced by the blockage on the peaks in the FRD. The FRD of the system is extracted in Fig. 2, where Eq. (1) is applied to the resultant transient response. The input and output from the system are the discharge perturbation generated by the movement of the side discharge valve located at the downstream end and the measured head perturbation at the valve for the duration of the transient signal, respectively (see Fig. 1). Details concerning the extraction of the FRD can be found in Lee et al. (2004b, 2005). The FRD of a pipeline system contains a series of regular harmonic peaks, spaced according to the fundamental frequency of the system. Fig. 2 shows that for a blockagefree system, the magnitudes of the peaks in the FRD are uniform, whereas a blockage within the system induces a sinusoidal-like oscillation on the peaks of the FRD. The following section shows the analytical expression for this oscillation that can be used to locate the blockage.

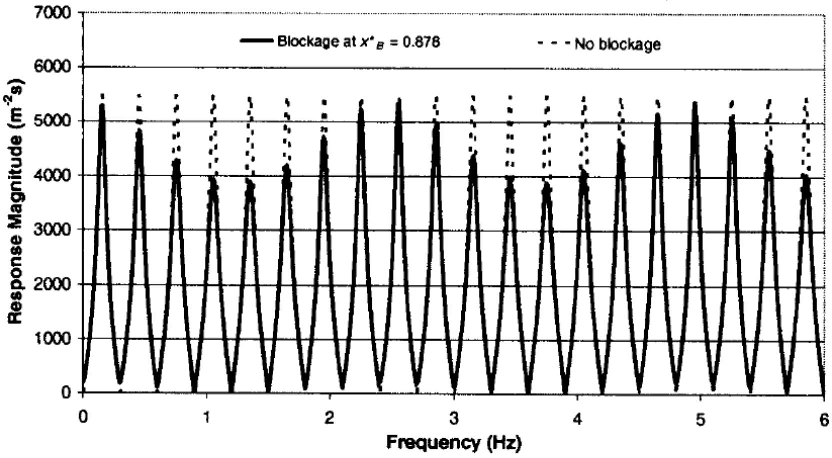

Figure 2: FRD of the blocked and intact pipeline shown in Fig. 1 generated from the transfer matrices

Impact of Blockage on the Peaks of the FRD

Given a pipeline system excited at a particular angular frequency, ω, the prediction of the head response at any point is given by the linearized transfer matrix equation (Chaudhry 1987; Wylie and Streeter 1993). Lee et al. (2005) present analysis relating to the Fig. 1. Pipeline system under consideration Fig. 2. FRD of the blocked and intact pipeline shown in Fig. 1 generated from the transfer matrices validity of the linear assumption in unsteady pipeline systems. The transfer matrix method uses a series of individual matrices, each corresponding to an element within the pipeline system. These matrices are multiplied in the order of their location starting from the downstream end to produce an overall transfer matrix of the pipe system, U [see Eq. (3)]. Combined with known boundary conditions, this overall transfer matrix is then solved for the complex discharge and head perturbations (*q* and *h*) at the extremities of the pipeline. The third row and the third column of this matrix are included to cater for external head and discharge perturbations imposed on the system

$$\begin{Bmatrix} q \\ h \\ 1 \end{Bmatrix}^{n_5} = \begin{bmatrix} U_{11} & U_{12} & U_{13} \\ U_{21} & U_{22} & U_{23} \\ U_{31} & U_{32} & U_{33} \end{bmatrix} \begin{Bmatrix} q \\ h \\ 1 \end{Bmatrix}^{n_1} \tag{3}$$

where, n_1, n_5 denote the position in the system of Fig. 1; *q*, *h*=discharge and head perturbations; and U_{ij}=(i, j)th entry in the system transfer matrix, *U*. Eq. (3), once solved, can be used to determine the head and discharge perturbations at any point within the system. Expanding Eq. (3) gives

$$q_{n_5} = U_{11}q_{n_1} + U_{12}h_{n_1} + U_{13} \tag{4}$$

$$h_{n_5} = U_{21}q_{n_1} + U_{22}h_{n_1} + U_{23} \tag{5}$$

The orifice equation (in a linearized form) relates the head loss (ΔH_{V0}) and discharge (Q_{V0}) through the side-discharge valve as

$$h_{n_5} = \frac{2\Delta H_{V0}}{Q_{V0}} q_{n_5} \tag{6}$$

Note that the head perturbation at the upstream reservoir is zero (h_{n1}=0). An expression for the head perturbation upstream of the valve based on the elements of the overall transfer matrix, *U*, is

$$h_{n_5} = \frac{\frac{2\Delta H_{V0}}{Q_{V0}}}{1 - \frac{2\Delta H_{V0}}{Q_{V0}}\frac{U_{11}}{U_{21}}} \tag{7}$$

As mentioned previously, the elements of the transfer matrix, *U*, can be determined by multiplying the individual matrices for each hydraulic element together, starting from the downstream boundary. The matrix for pipe sections can be found in Chaudhry (1987). To isolate the blockage-induced impact on the FRD, these are considered as frictionless units. The behavior of a discrete blockage can be considered as similar to an inline valve, and has the transfer matrix of the form

$$\begin{Bmatrix} q \\ h \\ 1 \end{Bmatrix}^{n_3} = \begin{bmatrix} 1 & 0 & 0 \\ -\dfrac{2\Delta H_{B0}}{Q_{B0}} & 1 & 0 \\ 0 & 0 & 1 \end{bmatrix} \begin{Bmatrix} q \\ h \\ 1 \end{Bmatrix}^{n_2} \tag{8}$$

where Q_{B0}, ΔH_{B0}=steady state flow through the blockage and the steady state head loss across the blockage, respectively. Formulation of the overall system transfer matrix and substituting U_{11} and U_{21} into Eq. (7) gives the frequency response measured at a position just upstream of the inline valve as

$$h_{n_5} = \frac{2\Delta H_{V0}}{Q_{V0} - \left(2\Delta H_{V0} \dfrac{\left[\dfrac{igA\Delta H_{B0}}{aQ_{B0}} + \dfrac{igA\Delta H_{B0}}{aQ_{B0}} \cos(2\pi x_B^* m - \pi x_B^*)\right]}{\left[\dfrac{-ia}{gA} + \dfrac{2\Delta H_{B0}}{Q_{B0}} \sin(2\pi x_B^* m - \pi x_B^*)\right]} \right)} \tag{9}$$

where *g*=gravitational acceleration; *a*=pipeline wave speed; *A*=cross-section pipe area; $i = \sqrt{-1}$; and the variable *m*=harmonic peak number in the FRD. For discrete blockages that do not result in a total constriction of the flow through the pipe, the term $2\Delta H_{B0}/Q_{B0}$ is small compared to $a/(gA)$ and Eq. (9) simplifies to

$$h_{n_5} = \frac{1}{\frac{1}{2}\left(\frac{\Delta H_{V0}}{Q_{V0}}\right)^{-1} + \left(\frac{a}{gA}\right)^{-2}\left(\frac{\Delta H_{B0}}{Q_{B0}}\right)(1 + \cos(2\pi x_B^* m - \pi x_B^*))} \tag{10}$$

Inverting the equation and defining I_B^* as the dimensionless blockage size, $B=a/gA$ as the pipe characteristic impedance, and $I_V=\Delta H_{V0}/Q_{V0}$ as the valve impedance gives an expression for the reciprocal of the peak magnitudes in the FRD as

$$\frac{1}{\left|h_{n_5}\right|} = \frac{1}{2I_V} + \frac{I_B^*}{B}(1 + \cos(2\pi x_B^* m - \pi x_B^*)) \tag{11}$$

where the frequency of the oscillation (in units of "per peak number") in the cosine function is given by x_B^* which is the coefficient to m, and the phase is πx_B^* , given by the remaining term. Eq. (9) indicates that a blockage induces a sinusoidal oscillation on the inverted peaks of the FRD. The properties of this blockage-induced oscillation are as follows:

- The frequency of the blockage-induced damping pattern from Eq. (9) is x_B^*, however, frequency aliasing means that for oscillation frequencies greater than the Nyquist frequency of 0.5, the signals will appear with frequencies of $(1-x_B^*)$. Each observed oscillation frequency in the peaks of the FRD can be caused by two possible frequencies, one above the Nyquist frequency and one below, indicating two possible blockage positions at mirror positions within the pipeline (Lee et al. 2003a).
- The phase of the blockage-induced damping pattern is πx_L^* and is also affected by possible aliasing, where aliased signals will display a reversed phase, $-\pi x_L^*$. The phase can be used to indicate whether the frequency underwent aliasing. The sign of the phase determines the correct blockage position from the two possible solutions found using the oscillation frequency. Signals with phase located in the first quadrant of the unit circle ($0 \leq$ phase $\leq \pi/2$) indicate a blockage in the up-stream half of the pipe and phases in the third quadrant ($-\pi/2 \geq$ phase $\geq -\pi$) indicate a blockage in the downstream half.
- The amplitude of the block-induced damping pattern is I_B^*/B, given in Eq. (9) as the coefficient to the blockage-generated cosine function, which can be used to determine the blockage size.

The extraction of the frequency, phase, and amplitude of the blockage-induced pattern from the inverted peaks of the FRD can be carried out using a Fourier transform, and is illustrated in the following section. The procedure for blockage detection is as follows:

1. Generate the FRD as described in Lee et al. (2005).

2. Extract the magnitudes of the peaks in the FRD and invert them.
3. Perform a Fourier transform of the inverted peak magnitudes to determine the frequency, phase, and amplitude of the blockage-induced pattern.
4. Use the frequency to determine the two possible blockage locations, then use the value of the phase to determine the correct location.
5. Using the amplitude of the oscillation, determine the magnitude of the blockage, given by I_B^*.

Note that the approximation made between Eq. (9) and Eq. (10) will generally induce only small errors in the prediction result. This is evident in Fig. 2 where the pattern created by a large blockage was shown to be sinusoidal even though the approximation was violated.

Numerical Validation of Blockage Detection Technique
The validation of the proposed blockage detection method is carried out for the pipeline system of Fig. 1. Three individual cases are considered with the blockage impedances and locations as given in Table 1. The head loss across the blockages are 1.15, 1.15, and 0.524 m for Case 1, 2, and 3, respectively, and the corresponding pipe flows are 1.07 x 10^{-2} m^3s^{-1}, 1.07 x 10^{-2} m^3s^{-1}, and 1.09 x 10^{-2} m^3s^{-1}. The peaks of the FRD for each blockage case are first inverted and then a Fourier transform performed, the result of which is shown in Fig. 3. For all cases, the oscillatory pattern in the inverted peaks has a frequency corresponding to either x_B^* or $(1-x_B^*)$. For a blockage located in the first half of the pipeline, the phase is in the first quadrant of the unit circle and for a blockage in the downstream half of the pipeline the phase is in the third quadrant. Using the blockage detection procedure, the blockage is correctly located for all three cases. The blockage sizes are also correctly determined. Note that a small discrepancy (approximately 0.5%) exists in the sizing of the blockage which is not evident in Table 1. This discrepancy is a result of the approximation made between Eqs. (9) and (10) which eliminated a small term from the equation, but the impact of which has no effect on the accuracy of the blockage location.

Table 1: Results of Single Blockage Detection

Case	True blockage properties		FRD peak pattern properties			Predicted blockage properties	
	Blockage position, x_B^*	Blockage size, I_B^*	Frequency (1/m)	Phase (rad)	Amplitude ($\times 10^{-5}$ m^2s^{-1})	Blockage position, x_B^*	Blockage size, I_B^*
1	0.878	0.062	0.122	-2.711	3.566	0.878	0.062
2	0.366	0.062	0.366	1.120	3.567	0.366	0.062
3	0.831	0.028	0.169	-2.500	1.600	0.831	0.028

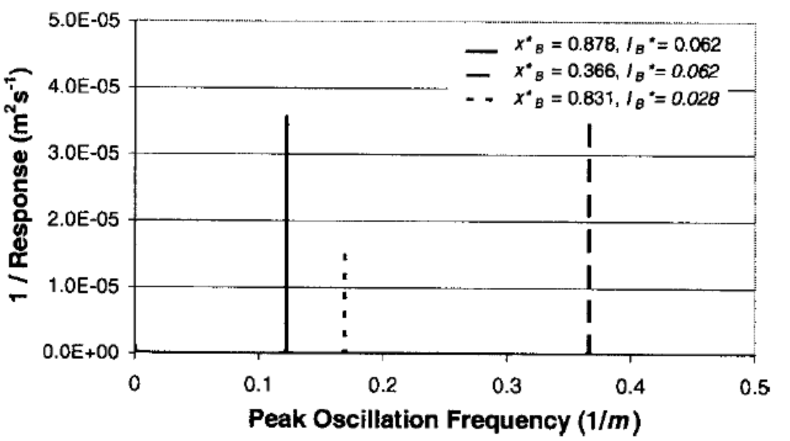

Figure 3: Spectrum of the inverted peaks magnitudes for three different blockage conditions

The blockage detection technique can also be expanded to cater for multiple blockages. In this case, Eq. (9) is rewritten as

$$\frac{1}{|h_{n_5}|} = \frac{1}{2I_V} + \frac{1}{B}\sum_{k=1}^{n_{block}} \left[I_{B_k}^* \left(1 + \cos\left(2\pi x_{B_k}^* m - \pi x_{B_k}^*\right)\right)\right] \quad (12)$$

where n_{block}=number of blocks in the system. The subscript k indicates the property is associated with the kth blockage. Eq. (10) shows that each blockage induces its own oscillatory pattern on the inverted peaks of the FRD, which can be separated in the Fourier spectrum as distinct impacts from the different blockages. This is illustrated in the multiple blockage example shown in Fig. 4. Two blocks, of size I_B^*=0.010, are located at two positions simultaneously within the pipeline, the details of which are shown in Table 2. The Fourier spectrum of the inverted FRD peaks in Fig. 4 indicates two frequencies, each associated with a particular blockage within the pipe. Applying the same procedure to each oscillation signal gives the correct position and size of the blocks as shown in Table 2. As in the single blockage case, excellent accuracy was shown for the location and sizing of the blockages within the system. Though not evident in Table 2, a slight error (approximately 1.1%) exists in the predicted blockage size. The prediction is not as accurate as in the case for a single blockage and is a result of the approximation made between Eqs. (9) and (10). Instead of eliminating one small term from the equation as in the case for a single blockage, the two blockages resulted in multiple omitted terms and the resultant error is therefore slightly greater than the case for a single blockage.

Table 2: Results of Multiple Blockage detection

	True blockage properties		FRD peak pattern properties			Predicted blockage properties	
	Blockage position, x_B^*	Blockage size, I_B^*	Frequency (1/m)	Phase (rad)	Amplitude (x10^{-5} m^2s^{-1})	Blockage position, x_B^*	Blockage size, I_B^*
Blockage 1	0.122	0.010	0.122	0.383	0.589	0.122	0.010
Blockage 2	0.183	0.010	0.183	0.575	0.579	0.183	0.010

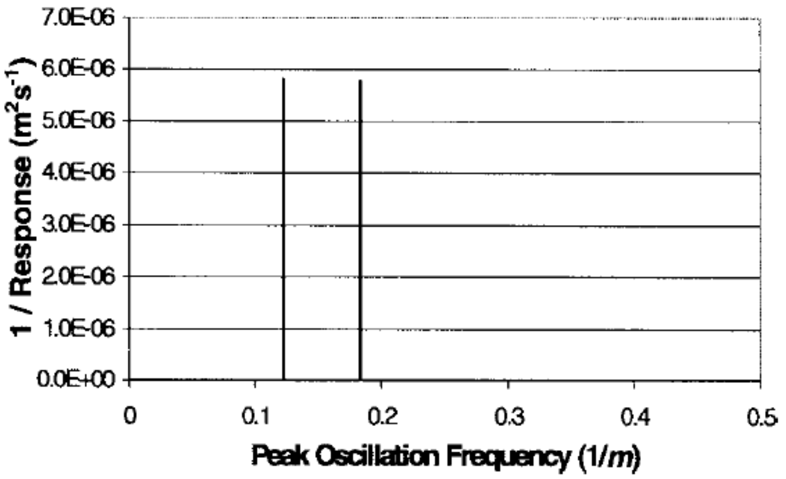

Figure 4: Spectrum of the inverted peaks magnitudes for a multiple blockage situation

Challenges in Real Systems

The technique assumes that the behavior of the blockage is similar to an inline orifice. In reality all blockages can have physical properties that deviate from this approximation. For example, the blockage may have a complicated geometry or is distributed along the length of the pipe. Only in systems where the length of the pipeline is long compared to the physical size of the blockage does the response of the blockage approach that of a discrete blockage, and the proposed technique can be applied to detect and to locate the problem.

The nature of the blockage pattern creates special cases where the proposed technique will fail. For example, two blockages at mirror locations in the pipeline will only be detected as one single blockage. In addition, when the blockage is located close to the system boundaries or the midpoint of the system, the resultant oscillation pattern on the peaks of the FRD will have a frequency close to zero, making the blockage difficult to detect. In these cases a combination of time domain analysis of the data and the proposed technique may be necessary to detect and locate the faults.

The application of the technique in a real system will require additional care with regards to the nature of the transient perturbation. The derivation presented in this paper assumes that the transient will be created using a side-discharge valve. This method for generating transients has been performed successfully in the field by other researchers (Stephens et al. 2005; Stoianov et al. 2003; Covas et al. 2004). However, the speed of the side-discharge valve maneuver must be fast to produce a signal that can excite a large number of modes (FRD peaks) in the system. In cases where this is not possible, the regression approach presented in Lee et al. (2004b) may be required to accurately determine the frequency and phase of the blockage induced pattern. Note that the proposed technique does not require the transient signal to be steady oscillatory but the signal must not be so large in magnitude that it will violate the assumption of linearity. Further details concerning the limits to the linearity approximations can be found in Lee et al. (2003b).

In a real pipeline situation the presence of other pipe fittings will create additional reflections in the transient trace, which in turn will result in additional oscillations in the FRD. These additional oscillations may be mistaken as blockages in the system and careful consultation with construction plans will be necessary to identify and remove these from the analysis.

The derivation presented in this paper assumes that the transient is generated and measured adjacent to the downstream valve boundary. Lee et al. (2005) has shown that this is the optimum system configuration and will lead to the maximum signal to noise ratio in the measured transient signal. In cases where this configuration cannot be met, a similar oscillation pattern will still be evident in the FRD, although the equation describing this pattern will deviate from Eq. (11). A similar approach to the one presented can be taken to derive the governing equation for these alternative configurations.

Another assumption in the derivation of Eq. (11) is that the system is frictionless, which may have implications for the technique when it is applied under real conditions. With the aid of correction procedures for the effects of steady and unsteady friction, Lee et al. (2004b) have used a similar FRD leak detection technique (derived with the same frictionless assumption) to accurately locate faults under experimental conditions. It is suspected that the same correction procedures can be used for the proposed blockage detection technique under real conditions but this should be verified in future studies.

The form of the derived Eq. (11) also provides insight into the operation of the technique. It is interesting to note that the frequency of the oscillatory pattern (the coefficient to "m" inside the cosine function) is affected only by the location of the blockage, x_B^*. The magnitude of the oscillatory pattern (the coefficient to the cosine term) is affected by a number of system parameters including the blockage size, wave speed, and the internal diameter. The mean about which the oscillation pattern takes place—the term that is added to the cosine function, a parameter that plays little part in the overall blockage detection process—is governed by the property of the boundary valve. These observations suggest that the proposed technique may be able to accurately locate the blockage (through an accurate determination of the oscillation frequency alone) even in a system where the system parameters (e.g., wave speed, internal diameter, valve characteristics) are not well known. Note that the technique will not be able to size the blockage under such conditions. A detailed parametric study may be required in future work to verify this finding.

Finally Eq. (11) was derived for a single pipeline system with specific boundary and system configurations. In the case of a network, Eq. (11) no longer applies and a similar procedure to the one presented in this paper will be required to derive the analytical expression for the blockage induced pattern on the FRD of the network. However, this approach is ambitious as the resultant expression will likely to be very complex compared to the form of Eq. (11) and this expression will also be specific to a particular network topology. Alternatively, Lee et al. (2005) presented a method where a complex system can be subdivided into individual single pipes and the FRD of each individual pipe segment within the network can be extracted. The blockage detection technique presented in this paper can therefore be applied to the resultant FRD of each pipe in the network. In order for this approach to work, a valve must exist at one extremity of the pipe to create a valve boundary and to partially isolate the pipe from the in Lee et al. (2005).

Conclusions

A procedure for blockage detection in a single pipeline using the FRD of the system is presented. A discrete blockage located within a single pipeline system is shown to generate an oscillatory pattern in the peaks of the FRD. The frequency, phase, and amplitude of this oscillation are related to the blockage location and size using an analytical expression derived using oscillatory unsteady flow equations. Once the FRD is extracted from the pipeline, the properties of the blockage-induced oscillations can be determined using a Fourier transform of the inverted peak magnitudes in the FRD. This technique is able to detect, locate, and size single or multiple discrete blockages. The approximation used in the derivation of the blockage detection equations was found to cause a small discrepancy in the estimation of the blockage size, but did not have any impact on the accuracy of the blockage location.

Notation

The following symbols are used in this technical note:

A = area of pipeline;
a = wave speed;
B = pipe characteristics impedance = *a/gA*;
C_V = valve loss coefficient;
g = gravitational acceleration;
H = hydraulic grade line elevation or frequency response function;
h = complex hydraulic grade line perturbation;
|*h*| = magnitude of head perturbation;
I_B = blockage impedance = $\Delta H_{B0}/Q_{B0}$;
I_B^* = dimensionless blockage size =I_B/B;
I_V = valve impedance = $\Delta H_{V0}/Q_{V0}$;
i = imaginary unit, $\sqrt{-1}$;
L = total length of pipeline;
L_A, L_B = lengths of pipe subdivided by the blockage;
m = harmonic peak number;
n_{block} = number of blockages within the pipeline;
Q = discharge;
Q_{B0} = steady state flow through the blockage;
Q_{V0} = steady state flow through the valve;
q = complex discharge perturbation;
t = time;
U = overall transfer matrix for the pipeline system excluding the boundary valve;
x = distance along pipe;
x_B^* = dimensionless position of blockage =xB/L;
ΔH_{B0} = steady state head loss across the blockage;
ΔH_{V0} = steady state head loss across the valve; and
ω = angular frequency.

References

1. Chaudhry, M. H. (1987). *Applied hydraulic transients*, Van Nostrand Reinhold, New York.
2. Covas, D., Ramos, H., Brunone, B., and Young, A. (2004). "Leak detection in water trunk mains using transient pressure signals: Field tests in Scottish water." *9th Int. Conf. on Pressure Surges*, BHR Group, Chester, U.K., 185–198.
3. De Salis, M. H. F., and Oldham, D. J. (2001). "The development of a rapid single spectrum method for determining the blockage characteristics of a finite length duct." *J. Sound Vib.*, 243(4), 625–640.
4. Lee, P., Vitkovský, J., Lambert, M., Simpson, A., and Liggett, J. (2005). "Frequency domain analysis for detecting pipeline leaks." *J. Hydraul. Eng.*, 131(7), 596–604.
5. Lee, P. J., and Vitkovský, J. P. (2006). "Discussion of 'Detection of partial blockage in single pipelines by P. K. Mohapatra, M. H. Chaudhry, A. A. Kassem, and J. Moloo.'" *J. Hydraul. Eng.*, accepted.
6. Lee, P. J., Vitkovský, J. P., Lambert, M. F., Simpson, A. R., and Liggett, J. A. (2003a). "Frequency response coding for the location of leaks in single pipeline systems." *Int. Conf. on Pumps, Electromechanical Devices and Systems Applied to Urban Water Management*, International Association of Hydraulic Research (IAHR) and International Water Association (IWA), Valencia, Spain.
7. Lee, P. J., Vitkovský, J. P., Lambert, M. F., Simpson, A. R., and Liggett, J. (2003b). "Discussion of 'Leak detection in pipes by frequency response method using a step excitation by Witness Mpesha, M. H. Hanif Chaudhry, and Sarah L. Gassman.'" *J. Hydraul. Res.*, 40(1), 2003, pp. 55–62.
8. Lee, P. J., Vitkovský, J. P., Lambert, M. F., Simpson, A. R., and Liggett, J. A. (2004). "Experimental validation of frequency response coding for the location of leaks in single pipeline systems." The Practical Application of Surge Analysis for Design and Operation, *9th Int. Conf. on Pressure Surges*, BHR Group, Chester, U.K., 239–253.
9. Lynn, P. (1982). *An introduction to the analysis and processing of signals*, Macmillan, London.
10. Mermelstein, P. (1967). "Determination of the vocal-tract shape from measured format frequencies." *J. Acoust. Soc. Am.*, 41_5), 1283–1294.

11. Mohapatra, P. K., Chaudhry, M. H., Kassem, A. A., and Moloo, J. (2006). "Detection of partial blockage in single pipelines." *J. Hydraul. Eng.*, 132(2), 200–206.
12. Schroeder, M. R. (1967). "Determination of the geometry of the human vocal tract by acoustic measurements." *J. Acoust. Soc. Am.*, 41, 1002–1010.
13. Stephens, M., Simpson, A. R., Lambert, M. F., and Vitkovský, J. P. (2005). "Field measurements of unsteady friction effects in a trunk transmission pipeline." *7th Annual Symp. on Water Distribution Systems Analysis*, ASCE, Anchorage, Alaska.
14. Stoianov, I., Maksimovic, C., Graham, N., and Dellow, D. (2003). "Field validation of the application of hydraulic transients for leak detection in transmission pipelines." *Advances in Water Supply Management*, Computing and Control for Water Industry (CCWI) '03, London, 86–97.
15. Vitkovský, J. P., Bergant, A., Lambert, M. F., and Simpson, A. R. (2003). "Unsteady friction weighting function determination from transient responses." *Pumps, electromechanical devices and systems applied to urban water management*, E. Cabrera and E. Cabrera, Jr., eds., Vol. II, Valencia, Spain, 781–789.
16. Wang, X.-J., Lambert, M. F., and Simpson, A. R. (2005). "Detection and location of a partial blockage in a pipeline using damping of fluid transients." *J. Water Resour. Plann. Manage.*, 131_3), 244–249.
17. Wylie, E. B., and Streeter, V. L. (1993). *Fluid transients in systems*, Prentice-Hall, Englewood Cliffs, N.J.